NANO LETTERS

2007
Vol. 7, No. 8
2211−2213

Nonlocal Exchange Interaction Removes Half-Metallicity in Graphene Nanoribbons

Elias Rudberg, Paweł Sałek,* and Yi Luo

Department of Theoretical Chemistry, Royal Institute of Technology, AlbaNova, S-106 91 Stockholm, Sweden

Received March 13, 2007; Revised Manuscript Received May 28, 2007

ABSTRACT

Band gap studies of zigzag-edge graphene ribbons are presented. While earlier calculations at LDA level show that zigzag-edge graphene ribbons become half-metallic when cross-ribbon electric fields are applied, our calculations with hybrid density functional demonstrate that finite graphene ribbons behave as half-semiconductors. The spin-dependent band gap can be changed in a wide range, making possible many applications in spintronics.

Properties of single-layer graphene have attracted much attention recently in both experimental[1−3] and theoretical[4−7] research. This compound is a very promising candidate material for future applications in nanoelectronics and molecular devices. Son, Cohen, and Louie[5,6] have reported ground-breaking ab initio theoretical investigations predicting a new fascinating property of graphene: zigzag-edge graphene nanoribbons may become half-metallic when an external electric field is applied across the ribbon. A half-metallic material shows a band gap in one spin direction, while the band gap in the other spin direction is zero.[5] Such materials are of great interest in spintronics applications,[5,8−10] where spin-polarized currents are desired. The calculations of Son, Cohen, and Louie[5,6] were done using periodic ab initio density functional theory (DFT) calculations at the local density approximation (LDA) level of theory. LDA by its construction neglects nonlocal exchange effects, which may play an important role in spin systems. Here we show that inclusion of a fractional Hartree−Fock exchange contribution through the hybrid B3LYP functional gives qualitatively different results: at a certain field strength, the nanoribbon system goes into a different electronic state so that half-metallicity is never reached for any strength of the cross-ribbon electric field. This means that graphene ribbons may not be half-metallic but instead behave as spin-selective semiconductors. One of the reasons for limited applicability of ordinary hybrid functionals in solid-state studies is the large evaluation cost of long-range distance HF exchange.[11] It has been however established that hybrid functionals provide better band gap predictions than pure functionals, particularly for small band gap systems.[12] The nonlocal exchange term in functionals can lead to an overestimation to the exchange splitting in metals. It is worth noting that this problem is less severe in B3LYP functional than in the PBE0 hybrid functional presented in that paper. For example, for graphene of width 4 and length 11, PBE0 functional with 6-31G* basis set predicts a band gap of 0.83 eV, while B3LYP gives a more realistic 0.58 eV. In another study, the HSE screened hybrid functional correctly predicts semiconducting behavior in systems where pure functionals erroneously predict a metal.[13]

We have carried out electronic structure calculations of graphene nanoribbons for varying external electric fields using three different exchange-correlation functionals: LDA, BLYP, and B3LYP. Our model systems are finite pieces of zigzag-edge graphene nanoribbons. The model system used in this work is a zigzag graphene nanoribbon with 8 zigzag chains (8-ZGNR) of length 7.1 nm, formula $C_{472}H_{74}$, see Figure 1. The molecule is completely flat, forming a perfect honeycomb pattern with C−C distance 1.42 Å and C−H distance 1.01 Å. Calculations on model systems of different lengths have shown that the band gaps are well converged at length 7.1 nm. This study was done for fixed geometry as described above. For smaller ZGNR systems, we have compared band gaps in fixed structures to the band gaps computed for optimized structures and found no significant differences. It appears the geometry is not critical for the resulting band gaps in this kind of calculations and this range of electric field strengths.

The self-consistent field (SCF) calculations reported in this work were carried out using the quantum chemistry program *ergo*,[14] which is focused on large-scale SCF calculations by applying Kohn−Sham DFT formalism. The program uses

* Corresponding author. E-mail: pawsa@theochem.kth.se.

10.1021/nl070593c CCC: $37.00
Published on Web 06/29/2007

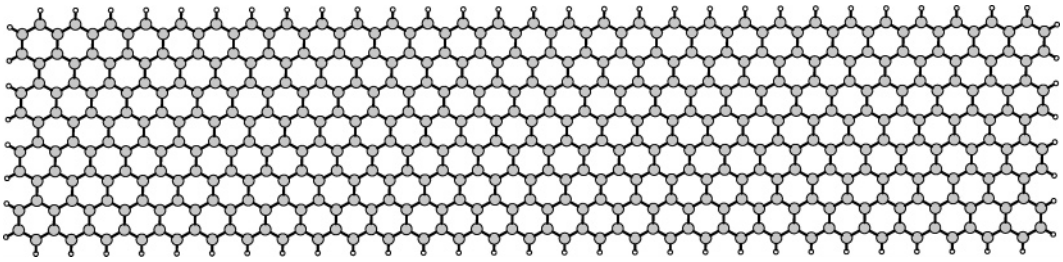

Figure 1. Model system: a zigzag edge graphene nanoribbon with 8 zigzag chains (8-ZGNR) of length 7.1 nm and width 1.6 nm. Chemical formula: $C_{472}H_{74}$.

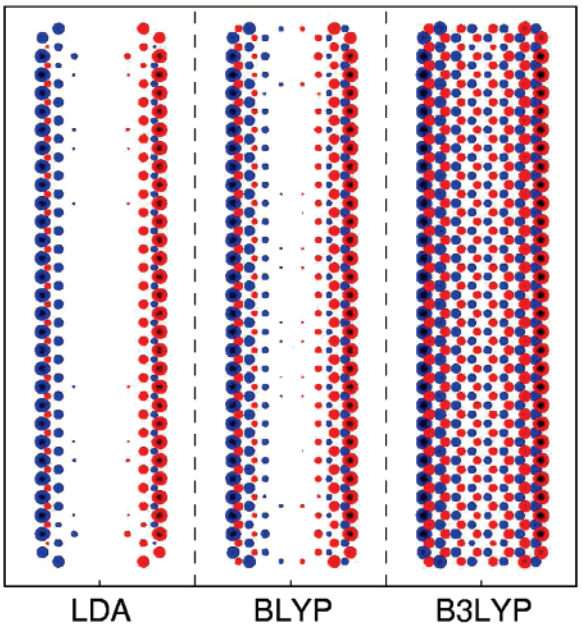

Figure 2. Graphs of spin density integrated in the direction perpendicular to the ribbon plane for zero external electric field. The spin density was calculated using different functionals and the 3-21G basis set. The color scale is such that dark-red/dark-blue corresponds to the largest spin density 0.47 $|e|$ Å^{-2}, smaller spin density is shown in lighter color, and spin density smaller than 0.025 $|e|$ Å^{-2} is neglected (white).

Gaussian type linear combination of atomic orbital basis functions; the 3-21G basis set was used for all the calculations reported, corresponding to 4396 basis functions for the studied nanoribbon model system.

Spin-unrestricted SCF calculations were performed for the 8-ZGNR model system, giving the spin density ($\rho_\alpha(\mathbf{r}) - \rho_\beta(\mathbf{r})$) and two separate gaps between highest occupied molecular orbital (HOMO) and lowest unoccupied molecular orbital (LUMO): one HOMO−LUMO gap for α electrons and one for β electrons. External electric fields of varying strength were applied across the ribbon, i.e., in the top-to-bottom direction in Figure 1. Figure 2 shows the computed spin density integrated in the direction perpendicular to the ribbon plane in the absence of external electric field. The spin density configuration is qualitatively similar in all three cases, with α- and β- spin alternating over the carbon atoms. The spin density's localization to the edges of the ribbon is most pronounced in the LDA case. We have also performed calculations for the corresponding ferromagnetic state (same spin on both edges). We find it has higher energy than the

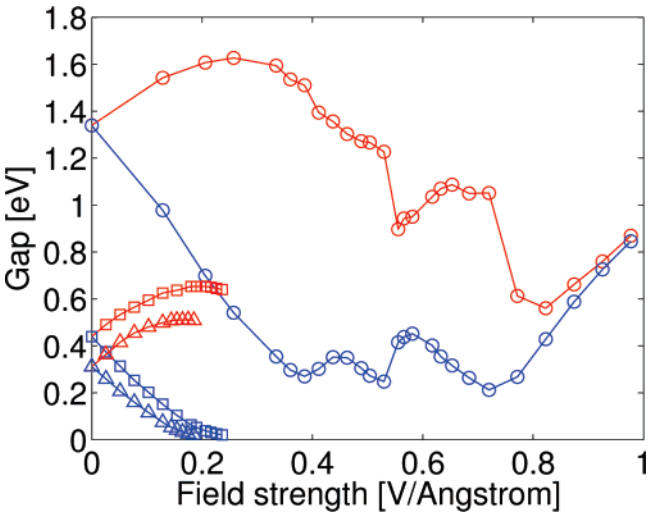

Figure 3. Computed band gaps plotted against external electric field, for a 8-ZGNR. The band gaps were calculated using the LDA, BLYP, and B3LYP functionals and the 3-21G basis set. LDA, BLYP, and B3LYP results are shown as triangles, squares, and circles, respectively. Note that for small field strengths the B3LYP behavior is the same as for LDA, but there is a marked change above 0.4 V Å^{-1}. See discussion in the text.

antiferromagnetic state that we focus on in this work. The computed total energy differences are 0.21, 0.22, and 0.77 eV for LDA, BLYP, and B3LYP, respectively. For LDA, this gives 1.8 meV per edge atom, in fairly good agreement with the value 2.0 meV per edge atom reported by Son, Cohen, and Louie.[5]

Our computed α and β HOMO−LUMO gaps are plotted in Figure 3 as functions of the external electric field for the three different functionals. We use the convention of labeling the larger gap as α and the smaller gap as β. The LDA curves are similar to the corresponding results of Son, Cohen, and Louie,[5,6] with gaps of 0.31 eV at zero field, and half-metallicity reached at around 0.20 V Å^{-1}. Our BLYP results are qualitatively similar to the LDA results, with small differences attributed to the addition of gradient corrections; the BLYP gaps are somewhat larger, 0.45 eV at zero field, and half-metallicity is reached at an electric field strength around 0.25 V Å^{-1}. For B3LYP, the gaps are much larger than those for the other functionals. At zero field, the B3LYP gaps are 1.34 eV. The gaps separate for small field strengths, but at around 0.4 V Å^{-1}, the trend changes. The β gap remains larger than 0.2 eV for all studied field strengths, and above 0.8 V Å^{-1}, the α- and β- gaps become almost the

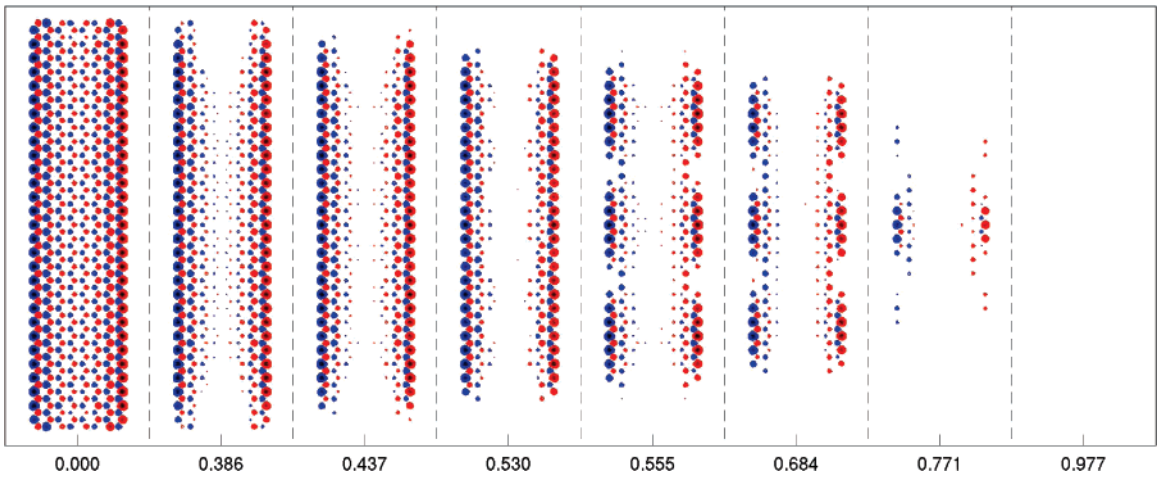

Figure 4. Graphs of spin density integrated in the direction perpendicular to the ribbon plane for different strengths of the external electric field. The spin density was calculated using the B3LYP functional and the 3-21G basis set. Field strengths are given below each image, in V Å^{-1}. The color scale is such that dark-red/dark-blue corresponds to the largest spin density 0.47 $|e|$ Å^{-2}, smaller spin density is shown in lighter color, and spin density smaller than 0.025 $|e|$ Å^{-2} is neglected (white).

same. Thus, the B3LYP functional does not predict the studied system to be half-metallic at any field strength.

To explain the B3LYP results in Figure 3, it is helpful to study how the spin density changes when the electric field is applied. Figure 4 shows the B3LYP spin density at eight different field strengths, indicating that several changes in the electronic state are responsible for the features of the band gap plot in Figure 3. For small field strengths, the spin density configuration differs only slightly from the zero-field case. But as the field gets stronger, the spin density is drastically reduced near the ends of the ribbon. This phenomenon seems to be related to the fact that the β band gap stops decreasing at the field around 0.4 V Å^{-1}. The discontinuity in the gaps at around 0.54 V Å^{-1} is clearly explained by the change to a qualitatively different electronic state, where the spin density is annihilated at two places along each ribbon edge, as shown in the 0.555 and 0.684 spin density graphs in Figure 4. It appears that nonlocal exchange interaction is responsible for this effect; the interaction reaches from one edge of the ribbon to the other edge. The next discontinuity, at around 0.75 V Å^{-1}, is related to the fact that the system approaches a spin-unpolarized (closed-shell) state for stronger external electric fields. We note that the spin density distributions obtained with LDA and BLYP functionals change only marginally for field strengths studied with these methods.

The observed change in electronic state shows that the choice of exchange-correlation functional is critical in theoretical investigations of this kind. On the basis of our B3LYP results, we find it uncertain whether half-metallicity can be achieved for graphene nanoribbons because our calculations give β gaps larger than 0.2 eV for all field strengths. This does not, however, make graphene less interesting for spintronics applications: the graphene ribbon should according to our calculations behave as a spin-selective semiconductor, and a spin-polarized current should appear if an appropriate gate voltage is applied together with the cross-ribbon electric field. Also, the cross-ribbon field should not be too strong, or the electronic state will change to a spinless state. Our B3LYP calculations predict the appropriate cross-ribbon electric field strength for maximum spin polarization of an 8-ZGNR to be in the range 0.4−0.8 V Å^{-1}.

Acknowledgment. This work is supported by the Swedish Research Council (V.R.).

References

(1) Novoselov, K. S.; Geim, A. K.; Morozov, S. V.; Jiang, D.; Zhang, Y.; Dubonos, S. V.; Grigorieva, I. V.; Firsov, A. A. *Science* **2004**, *306*, 666.
(2) Zhang, Y.; Jiang, Z.; Small, J. P.; Purewal, M. S.; Tan, Y.-W.; Fazlollahi, M.; Chudow, J. D.; Jaszczak, J. A.; Stormer, H. L.; Kim, P. *Phys. Rev. Lett.* **2006**, *96*, 136806.
(3) Novoselov, K. S.; Geim, A. K.; Morozov, S. V.; Jiang, D.; Katsnelson, M. I.; Grigorieva, I. V.; Dubonos, S. V.; Firsov, A. A. *Nature* **2005**, *438*, 197.
(4) Pereira, V. M.; Guinea, F.; Lopes dos Santos, M. B.; Peres, N. M. R.; Castro Neto, A. H. *Phys. Rev. Lett.* **2006**, *96*, 036801.
(5) Son, Y. W.; Cohen, M. L.; Louie, S. G. *Nature* **2006**, *444*, 347.
(6) Son, Y. W.; Cohen, M. L.; Louie, S. G. *Phys. Rev. Lett.* **2006**, *97*, 216803.
(7) Barone, V.; Hod, O.; Scuseria, G. E. *Nano. Lett.* **2006**, *6*, 2748.
(8) Wolf, S. A.; Awschalom, D. D.; Buhrman, R. A.; Daughton, J. M.; von Molnar, S.; Roukes, M. L.; Chtchelkanova, A. Y.; Treger, D. M. *Science* **2001**, *294*, 1488.
(9) Zutic, I.; Fabian, J.; Das Sarma, S. *Rev. Mod. Phys.* **2004**, *76*, 323.
(10) Durgun, E.; Senger, R. T.; Sevincli, H.; Mehrez, H.; Ciraci, S. *Phys. Rev. B* **2006**, *74*, 235413.
(11) Heyd, J.; Scuseria, G. E.; Ernzerhof, M. *J. Chem. Phys.* 2003, *118*, 8207.
(12) Paier, J.; Marsman, M.; Hummer, K.; Kresse, G.; Gerber, I. C.; Ángtán, J. G. *J. Chem. Phys.* **2006**, *124*, 154709.
(13) Heyd, J.; Peralta, J. E.; Scuseria, G. E.; Martin, R. L. *J. Chem. Phys.* **2005**, *123*, 174101.
(14) Rudberg, E.; Rubensson, E.; Sałek, P. *Ergo* version 1.1, a quantum chemistry program for large-scale self-consistent field calculations, 2006.

NL070593C